Cholesterol and Ergosterol Superlattices in Three-Component Liquid Crystalline Lipid Bilayers as Revealed by Dehydroergosterol Fluorescence

Fang Liu,* Istvan P. Sugar,# and Parkson Lee-Gau Chong*
*Department of Biochemistry, Temple University School of Medicine, Philadelphia, Pennsylvania 19140, and #Departments of Biomathematical Sciences and Physiology/Biophysics, The Mount Sinai School of Medicine, New York, New York 10029 USA

ABSTRACT We have examined the fractional sterol concentration dependence of dehydroergosterol (DHE) fluorescence in DHE/cholesterol/dimyristoyl-L-α-phosphatidylcholine (DMPC), DHE/ergosterol/DMPC and DHE/cholesterol/dipalmitoyl-L-α-phosphatidylcholine (DPPC) liquid-crystalline bilayers. Fluorescence intensity and lifetime exhibit local minima (dips) whenever the total sterol mole fraction, irrespective of the DHE content, is near the critical mole fractions predicted for sterols being regularly distributed in hexagonal superlattices. This result provides evidence that all three of these naturally occurring sterols (e.g., cholesterol, ergosterol, and DHE) can be regularly distributed in the membrane and that the bulky tetracyclic ring of the sterols is the cause of regular distribution. Moreover, at the critical sterol mole fractions, the steady-state anisotropy of DHE fluorescence and the calculated rotational relaxation times exhibit distinct peaks, suggesting that membrane free volume reaches a local minimum at critical sterol mole fractions. This, combined with the well-known sterol condensing effect on lipid acyl chains, provides a new understanding of how variations in membrane sterol content change membrane free volume. In addition to the fluorescence dips/peaks corresponding to hexagonal superlattices, we have observed intermediate fluorescence dips/peaks at concentrations predicted by the centered rectangular superlattice model. However, the 22.2 mol% dip for centered rectangular superlattices in DHE/ergosterol/DMPC mixtures becomes diminished after long incubation (4 weeks), whereas on the same time frame the 22.2 mol% dip in DHE/cholesterol/DMPC mixtures remains discernible, suggesting that although all three of these sterols can be regularly distributed, subtle differences in sterol structure cause changes in lateral sterol organization in the membrane.

INTRODUCTION

Lateral sterol organization is an important subject in membrane biology (reviewed in Schroeder et al., 1991; Hui, 1993). The evidence for sterols being regularly distributed into hexagonal superlattices in phospholipid bilayers was first reported from our laboratory (Chong, 1994). We found that the fractional concentration dependence of dehydroergosterol ($\Delta^{5,7,9,(11),22}$-ergostatetraene-3β-ol, DHE) fluorescence in the liquid-crystalline state of dimyristoyl-L-α-phosphatidylcholine (DMPC) multilamellar vesicles exhibits many distinct fluorescence intensity drops (referred to as DHE dips) at specific DHE mole fractions. Those mole fractions match the critical sterol mole fractions predicted by the extended hexagonal superlattice model (Tang and Chong, 1992; Chong, 1994).

DHE is a naturally occurring fluorescent sterol (Delseth et al., 1979), with physical and physiological properties resembling those of ergosterol and cholesterol (Rogers et al., 1979; Bar et al., 1989). Thus, based on the observation of DHE dips and the physical principles underlying lipid regular distribution that we learned from previous studies on pyrene-labeled phospholipid bilayers (Somerharju et al., 1985; Chong et al., 1994; Sugar et al., 1994), we have proposed a general model for sterol lateral organization in membranes (Chong, 1994). Our model includes the following essential elements:

1. Sterol molecules tend to be maximally separated and thus regularly distributed in a hexagonal lipid matrix.

2. The difference in cross-sectional area between the bulky steroid ring and the matrix phospholipid acyl chain causes an elastic deformation in the hexagonal lipid lattice. This deformation provides the driving force (a repulsive interaction between bulky moieties) for maximum separation of the bulky lipids (Virtanen et al., 1988; Tang and Chong, 1992; Sugar et al., 1994).

3. Because of thermal fluctuation, changes in vesicle curvature, and the presence of impurities, irregular distributions always coexist with regular distributions (Tang and Chong, 1992; Sugar et al., 1994).

4. The number of lipid molecules belonging to the regions of regular distributions reaches a local maximum at critical sterol mole fractions and a local minimum between two consecutive critical sterol mole fractions (Sugar et al., 1994).

5. Membrane free volume is more abundant in irregular regions than in regular regions (Chong et al., 1994).

6. In the regular region, sterol molecules are not embedded as deep in the bilayer as those in the irregular region.

7. The critical sterol mole fractions Y (or Y′) can be predicted from the extended hexagonal superlattice model (Tang and Chong, 1992; Chong, 1994). When the cross-sectional area of lipid acyl chain is greater than the cross-

Received for publication 6 December 1996 and in final form 21 February 1997.

Address reprint requests to Dr. Parkson L. G. Chong, Department of Biochemistry, Temple University School of Medicine, 3420 N. Broad St., Philadelphia, PA 19140. Tel: 215-707-4182; Fax: 215-707-7536; E-mail: plchong@vm.temple.edu.

0006-3495/97/05/2243/12 $2.00

sectional area of sterol, the critical sterol mole fraction Y is given by the equation

$$Y = 2/(n_a^2 + n_a n_b + n_b^2 + 1), \quad (1)$$

where n_a and n_b are two integer coordinates along the two principal axes a and b, respectively (Somerharju et al., 1985; Virtanen et al., 1988). When the relative sizes of the sterol and the acyl chain cross-sectional area are reversed (at ~30 mol% sterol at 35°C for sterol/DMPC mixtures), the critical sterol mole fraction Y′ is described as (Chong, 1994)

$$Y' = 1 - [2/(n_a^2 + n_a n_b + n_b^2)]. \quad (2)$$

The critical sterol mole fractions predicted by the original hexagonal (Virtanen et al., 1988) and the extended hexagonal (Tang and Chong, 1992; Chong, 1994) superlattice models are listed in Table 1.

Our sterol regular distribution model (Chong, 1994) agrees with the well-known cholesterol condensing effect on lipid acyl chains (Huang and Mason, 1982; Almeida et al., 1992; see discussion in Chong, 1994) and is not incompatible with currently proposed phase diagrams (Ipsen et al., 1987; Vist and Davis, 1990; Matteo et al., 1995; McMullen and McElhaney, 1995; see discussion in Chong et al., 1996a). The model is not incompatible with models of aligned sterol domains (Rogers et al., 1979) or homogeneous distributions (Hyslop et al., 1990) because in our model, regular and irregular regions coexist and sterols are aligned (figure 2 *A–C* in Chong, 1994) or homogeneously distributed (figure 2, *A* and *B*, in Chong, 1994) in the regular region. Moreover, our model is consistent with the direct volume measurement made by Melchior et al. (1980), who showed several local minima and maxima in the plots of partial specific volume versus mole fraction of cholesterol in the liquid-crystalline state of dipalmitoyl-L-α-phosphatidylcholine (DPPC). Furthermore, our original findings of evidence for regular sterol distribution have been supported by spectroscopic data obtained from other groups (Parasassi et al., 1995; Tang et al., 1995; Virtanen et al., 1995). Notably, Virtanen et al. (1995) reported not only hexagonal superlattices, but centered rectangular superlattices as well for cholesterol lateral distribution in DMPC bilayers. The critical sterol mole fraction, X, for centered rectangular superlattices can be calculated by the equation (Virtanen et al., 1995; Table 1)

$$X = 2/(n_b^2 + 2n_a n_b + 1). \quad (3)$$

Despite this supporting evidence, more tests are needed to verify the physical properties implicated by the sterol regular distribution model.

In the present study we have undertaken critical tests on the sterol regular distribution model. First, we have used three naturally occurring sterols, i.e., DHE (a fluorescent sterol found in a Red Sea sponge *Biemna fortis*; Delseth et al., 1979), cholesterol (the dominant sterol in mammalian cell membranes), and ergosterol (the dominant sterol in

TABLE 1 Comparison between the dips/peaks positions observed and theoretically predicted critical sterol mole fractions corresponding to the original hexagonal, extended hexagonal, and centered rectangular superlattice models

Critical sterol mol%			Observed dip/peak positions		
Original hexagonal*	Extended hexagonal#	Centered rectangular§	Anisotropy peak¶	Lifetime dip‖	Intensity dip**
50.0 (1,1)	50.0 (0,2)	50.0 (1,1)	50.0	ND	50.0
40.0 (0,2)	—	40.0 (0,2)	40.0	ND	43.0
—	33.3 (1,1)	33.3 (2,1)	35.0;32.0	ND	33.3
25.0 (1,2)	25.0 (1,2)	—	24.6	25.0	25.3
—	—	22.2 (1,2)	22.2	—	22.6
20.0 (0,3)	20.0 (0,3)	20.0 (0,3)	20.3	20.3	20.3
15.4 (2,2)	15.4 (2,2)	15.4 (2,2)	15.8	15.8	15.8
14.3 (1,3)	14.3 (1,3)	—	13.5	14.3	14.7
—	—	12.5 (1,3)	12.3	ND	—
11.8 (0,4)	11.8 (0,4)	11.8 (0,4)	11.8	ND	11.8
10.0 (2,3)	10.0 (2,3)	—	10.2	ND	10.8;9.6
9.1 (1,4)	9.1 (1,4)	9.1 (2,3)	—	ND	9.0
—	—	8.0 (1,4)	—	ND	—
7.7 (0,5)	7.7 (0,5)	7.7 (0,5)	—	ND	7.7
7.1 (3,3)	7.1 (3,3)	7.1 (3,3)	—	ND	ND
6.9 (2,4)	6.9 (2,4)	—	—	ND	ND
6.3 (1,5)	6.3 (1,5)	—	—	ND	ND
—	—	6.1 (2,4)	6.0	ND	ND

*The values of critical sterol mol% were calculated from Eq. 1 with n_a, n_b values indicated within the parentheses.
#The values were calculated from Eq. 1 (for <30 mol%) and Eq. 2 (for >30 mol%).
§The values were calculated from Eq. 3.
¶The values were taken from Fig. 6.
‖The values were taken from Fig. 5 *A*.
**The values were taken from Fig. 4.
ND, Not determined. The dash means that the expected dips/peaks were not found.

fungal cell membranes), as membrane components to test the idea that the rigid and bulky tetracyclic ring of the sterol is the cause of sterol regular distribution in phospholipid matrix. Second, we have used the lifetime data of DHE fluorescence to verify the model that, in the regular region, sterols are not embedded as deep in the bilayer as those in the irregular region. Third, we have measured the sterol concentration dependence of steady-state anisotropy of DHE fluorescence in DHE/cholesterol/DMPC, DHE/cholesterol/DPPC, and DHE/ergosterol/DMPC mixtures to test the idea that membrane free volume reaches a local minimum at critical sterol mole fractions. Our lifetime, anisotropy, and intensity data all reveal peculiar behaviors at critical sterol mole fractions, showing that this kind of fluorescence evidence for sterol regular distribution exists not only in two-component (Chong, 1994; Virtanen et al., 1995; Parassasi et al., 1995; Chong, 1996; Chong et al., 1996a,b) but also in three-component membranes, irrespective of the type of sterols. Fourth, we have determined the reproducibilities, stabilities, and fluctuations of DHE dip positions at different sample incubation times. Last, we found that sterols can be arranged in hexagonal or centered rectangular superlattices. However, some centered rectangular superlattices are metastable relative to hexagonal superlattices in DHE/ergosterol/DMPC mixtures; in contrast, this metastability is not obvious in DHE/cholesterol/DMPC mixtures, suggesting that subtle differences in sterol conformations cause changes in sterol lateral organization in membranes. Based on these new findings and our earlier works on sterol regular distribution (Chong, 1994, 1996; Chong et al., 1996a,b), a putative functional role of membrane sterol content is proposed.

MATERIALS AND METHODS

Materials

DHE and cholesterol were obtained from Sigma (St. Louis, MO). Ergosterol was obtained from Matreya (Pleasant, PA). Cholesterol and ergosterol were recrystalized from ethanol. DHE was purified by high-performance liquid chromatography with a C-18 reverse-phase column (3.9 mm × 150 mm, μ-Bondapak; Millipore, Marlboro, MA), using methanol/acetonitrile (67:33, v/v) as the mobile phase. DMPC and DPPC were purchased from Avanti Polar Lipids (Alabaster, AL) and used as such. The concentration of DHE was determined using an extinction coefficient at 326 nm equal to 10,600 M^{-1} cm^{-1} (in dioxane) (Muczynski and Stahl, 1983). The phospholipid concentration was determined by the method of Bartlett (1959).

Preparation of liposomes

Appropriate amounts of sterols and phospholipids were first mixed in chloroform. The mixture was then dried under nitrogen in microtubes (Perfector Scientific, Atascadero, CA) and placed under high vacuum overnight. The dried mixtures were suspended in 10 mM Tris at pH 7.5. The dispersion was vortexed for 3 min at temperatures (~40°C for DMPC and 56°C for DPPC) well above the main phase transition temperatures of the matrix phospholipids. The samples were cooled to 4°C for 30 min and then incubated at 40°C for 30 min for vesicles containing DMPC or at 56°C for 30 min for vesicles containing DPPC. This cooling/heating cycle was repeated two more times. Finally, the samples were stored at room temperature (~25°C) for at least 4 days before fluorescence measurements.

Note that heating/cooling cycles and long incubation have frequently been used in liposome preparations for calorimetric studies (e.g., Lin and Huang, 1988; Mason, 1994). This protocol provides a means of evenly distributing membrane components among lipid multilayers and attaining an equilibrium distribution of molecules within each monolayer. Since 1987 our laboratory has routinely used this protocol to prepare lipid vesicles for fluorescence studies (e.g., Kao et al., 1990). Furthermore, when we studied the PyrPC (1-palmitoyl-2-(10-pyrenyl)decanoyl-*sn*-glycerol-3-phosphatidylcholine) concentration dependence of excimer/monomer (E/M) in 1991–92, we conducted the experiment at small PyrPC concentration intervals (~0.5–1.0 mol%) over a wide concentration range, in an attempt to improve the global analysis of PyrPC fluorescence data (Sugar et al., 1991). Because we employed cooling/heating cycles and long incubation and small concentration intervals, we observed *E/M* dips (Tang and Chong, 1992). Using these procedures, we also discovered DHE fluorescence intensity dips (Chong, 1994) and diphenylhexatriene (DPH) fluorescence polarization peaks (Chong, 1996; Chong et al., 1996a) at critical sterol mole fractions. Without these procedures, smooth variations of fluorescence parameters with sterol concentration were previously reported by others (e.g., Schroeder et al., 1987).

Fluorescence measurements

Fluorescence intensity measurements were made with an SLM DMX-1000 fluorometer (SLM Instruments, Urbana, IL). Samples were excited at 325 nm with a 2-nm bandpath. The emission was observed through a monochromator with an 8-nm bandpath. The concentration of lipids used for fluorescence measurements was ~2 mM. Blank readings from vesicles in the absence of DHE were negligible.

Steady-state anisotropy measurements were made on an ISS K2 fluorometer (ISS, Champaign, IL) using an L-format optical arrangement. The excitation wavelength used was 325 nm, with a bandwidth of 8 nm. Emission was collected through a Schott KV389 cutoff filter. Blank readings from membranes without probes were subtracted from the sample readings.

Fluorescence lifetimes were determined by using an ISS K2 phase-modulation fluorometer. The light source was a He-Cd laser (model 4240NB; LiConix, Sunnyvale, CA). The excitation used was 325 nm. The excitation polarizer was set at 35°C with respect to the vertical plane, and no emission polarizer was used. Phase and modulation values were determined relative to a *p*-bis[2-(5-phenyloxazolyl)]benzene (POPOP) (in ethanol) reference solution, which has a lifetime of 1.35 ns (Lakowicz et al., 1981) at 325-nm excitation. A Schott KV-389 cutoff filter was used for DHE emission intensity decay measurements. The emission decay data were analyzed with the software provided by ISS. For all of the fluorescence measurements, the temperature of the sample was controlled by a circulating bath.

RESULTS

Effect of total sterol content on DHE intensity dips

Fig. 1, *A* and *B*, shows the fractional sterol concentration dependence of dehydroergosterol (DHE) fluorescence intensity in DHE/ergosterol/DMPC multilamellar vesicles at 35°C. When the mol% of DHE was fixed at 5 mol%, two major DHE dips (indicated by *arrows* in Fig. 1 *A*) were observed at 20.0 and 25.6 mol% total sterol in the concentration range examined (17–28 mol%). Sterol total mol% = mol% DHE + mol% ergosterol. These two concentrations are close to the critical sterol mole fractions (i.e., 20 and 25 mol%, Table 1) predicted for sterols regularly distributed in

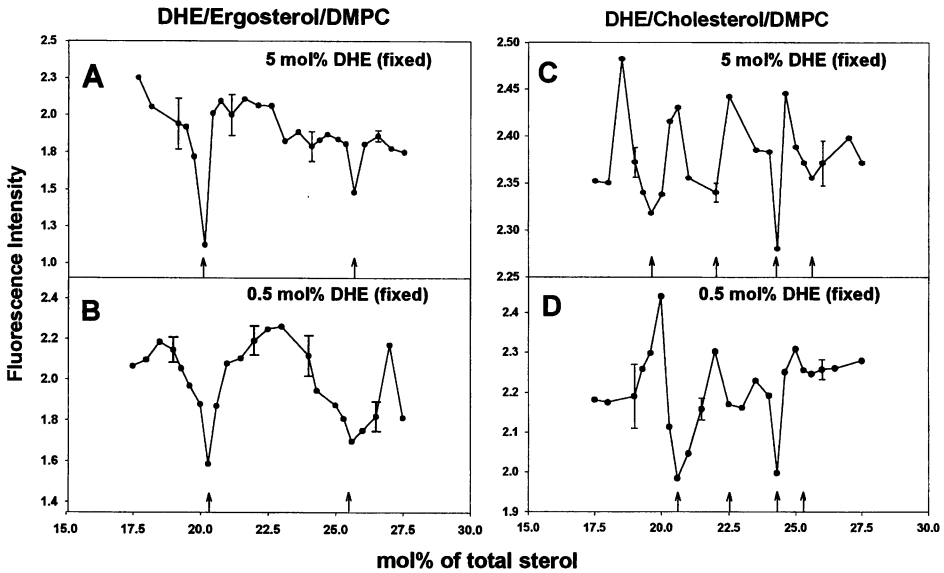

FIGURE 1 Sterol concentration dependencies of DHE fluorescence intensity (measured at 35°C while stirring) in DHE/ergosterol/DMPC (*A* and *B*) and DHE/cholesterol/DMPC (*B* and *C*) multilamellar vesicles. Fluorescence intensity was measured from 350 to 450 nm. DHE was fixed at 5 (*A* and *C*) or 0.5 (*B* and *D*) mol%. Error bars were determined from three independently prepared samples (error bars in other figures bear the same meaning). Before fluorescence measurements, the samples were incubated at room temperature for 7 days (referred to as the sample incubation time).

hexagonal superlattices (Chong, 1994) (note from Table 1 that 20 mol% is also a critical sterol mole fraction predicted by the centered rectangular model; Virtanen et al., 1995). When DHE was lowered to 0.5 mol%, two distinct DHE intensity dips were still observed at similar positions, i.e., 20.3 and 25.6 mol% total sterol (indicated by *arrows* in Fig. 1 *B*). Comparing these dips with the 20 and 25 mol% DHE dips previously observed from DHE/DMPC binary mixtures (Chong, 1994), it becomes apparent that the mixing ratio of DHE (fluorescent) to ergosterol (nonfluorescent) is unimportant for generating DHE dips. As long as the total sterol content is near the critical mole fraction, a distinct DHE intensity dip is observed. The observation that DHE dips are still clearly observable when the mole fraction of DHE is lowered from 5 to 0.5 mol% (Fig. 1 *B*) indicates that the original findings of DHE dips (Chong, 1994) are not a fluorescence artifact due to the use of high DHE mole fractions.

Fig. 1, *C* and *D*, shows a similar effect in DHE/cholesterol/DMPC multilamellar vesicles at 35°C. In this case, sterol total mol% = mol% DHE + mol% cholesterol. When the DHE content was fixed at 5 mol%, four prominent intensity dips were noticed at 19.6, 22.0, 24.3, and 26.0 mol% total sterol in the concentration range examined (Fig. 1 *C*). Similar dips were detected at 20.6, 22.5, 24.3, and 26.0 mol% total sterol when the DHE content was lowered to 0.5 mol% (Fig. 1 *D*). The dips near 25 and 22 mol% can be attributed to the formation of hexagonal superlattices and centered rectangular superlattices, respectively (Table 1). The dip near 20 mol% can be predicted by either the hexagonal or the centered rectangular superlattice model (Table 1). The physical origin of the small dip at ~26 mol% is not clear.

Stability of DHE intensity dips

Fig. 2 *A* shows DHE intensity dips (indicated by *arrows*) obtained from DHE/ergosterol/DMPC mixtures incubated at room temperature (~25°C) for 7 days. The dips at 15.4 and 20.0 mol% total sterol are expected from either the hexagonal or the centered rectangular superlattice model, whereas the dip at 22.6 mol% is close to the critical sterol mole fraction of 22.2 mol%, predicted only from the centered rectangular superlattice model, and the 25.0 mol% dip is predicted only from the hexagonal superlattice model (Table 1). Interestingly, after a prolonged incubation at room temperature (4 weeks), the 22.6 mol% dip disappears and only the dips resulting from hexagonal superlattices (e.g., 15.4, 20.0, and 25.0 mol%) are retained (Fig. 2 *B*). Apparently, in DHE/ergosterol/DMPC mixtures, the centered rectangular superlattices corresponding to the 22.2 mol% dip are metastable. Similar results were observed in DHE/DMPC mixtures (Chong, unpublished results).

However, the effect of vesicle incubation on DHE dips in DHE/cholesterol/DMPC mixtures is different from that in DHE/ergosterol/DMPC mixtures. Fig. 2 *C* shows the DHE intensity dips obtained from DHE/cholesterol/DMPC mixtures using the samples incubated at room temperature for 7 days. Four local minima (e.g., 19.3, 21.5, 25.3, and 26.5 mol%, indicated by *arrows* in Fig. 2 *C*) were detected. These minima, including the dip at ~22 mol%, remained distinctly discernible after 4 weeks of incubation at room temperature (Fig. 2 *D*). This result suggests that in DHE/cholesterol/DMPC mixtures and within the time frame of 4 weeks, both centered rectangular and hexagonal superlattices are stable, a result in contrast to that obtained from DHE/ergosterol/DMPC (Fig. 2, *A* and *B*).

Reproducibility of DHE intensity dips

As shown in Figs. 1 and 2, in the range of 17–28 mol% total sterol, DHE intensity dips can be detected in the neighborhood of 20, 22.2, 25, and 26.5 mol% total sterol in both DHE/ergosterol/DMPC and DHE/cholesterol/DMPC mixtures. However, the reproducibilities of each of these four

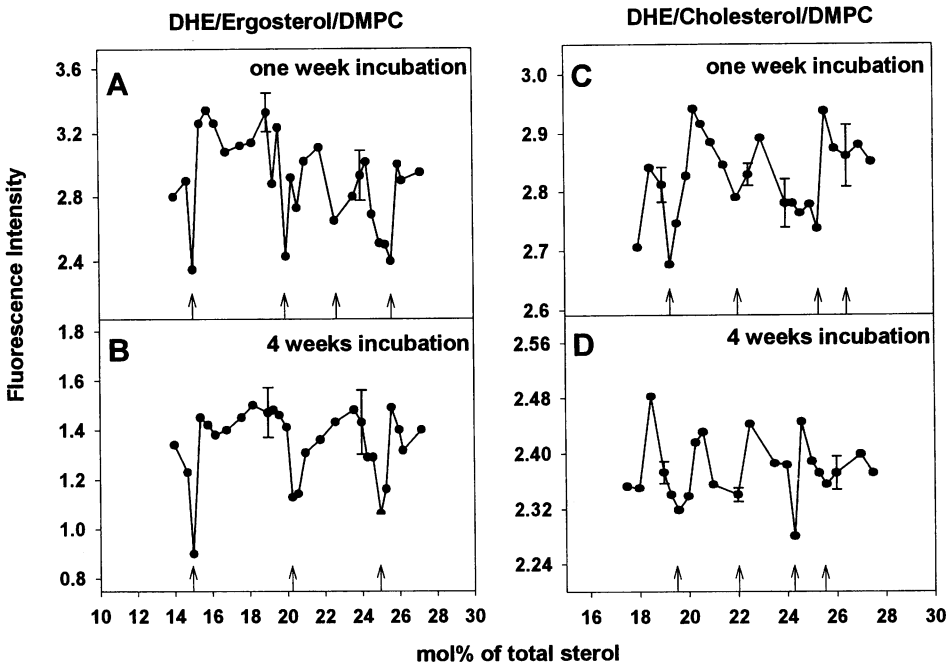

FIGURE 2 Effect of incubation time on DHE intensity dips, measured at 35°C while stirring, in DHE/ergosterol/DMPC (*A* and *B*) and DHE/cholesterol/DMPC (*C* and *D*) multilamellar vesicles. DHE was fixed at 0.5 mol%. Sample incubation times were 7 days (*A* and *C*) or 28 days (*B* and *D*).

dips may depend on the incubation time (Table 2). For example, the DHE intensity dips in the neighborhood of 20 and 25 mol% total sterol in DHE/ergosterol/DMPC mixtures are always detectable (from 13 sets of independently prepared samples) regardless of incubation time. However, the reproducibilities of the dips in the neighborhood of 22.2 and 26.5 mol% total sterol are dependent upon the incubation time. The reproducibilities of these two dips are less than 23% for the samples incubated at room temperature for 7 days, and become even lower after 28 days' incubation, with a virtually zero reproducibility for the 22.2 mol% dip. In contrast, the reproducibility of the 22.2 mol% dip in DHE/cholesterol/DMPC mixtures is near 100%, irrespective of incubation time (Table 2). As in the case of DHE/ergosterol/DMPC, the reproducibilities of the dips in the neighborhood of 20 and 25 mol% total sterol in DHE/cholesterol/DMPC mixtures are near 100% (determined from 16 sets of independently prepared samples).

Fluctuations of DHE intensity dip positions

Fig. 3, *B* and *D*, shows the fluctuations of the dip positions in the neighborhood of 20 and 25 mol% total sterol, respectively, in DHE/ergosterol/DMPC mixtures. More precisely, DHE intensity dips were measured at 19.3, 19.6, 20.0, 20.3, 20.6 and at 24.3, 24.6, 25.0, 25.3, 25.6 mol% total sterol. The frequency of appearance (%) of dips at these particular total sterol concentrations was determined from 13 sets of independently prepared samples. DHE dips are not always observed exactly at the critical sterol mole fractions predicted by the hexagonal or the centered rectangular superlattice model. However, the distributions of the dip positions are centered around the predicted critical sterol mole fractions, i.e., 20 and 25 mol%. The distribution appears to be random, with a small fluctuation of <0.4 mol%. Similar results were obtained from 16 sets of DHE/cholesterol/DMPC mixtures (Fig. 3, *A* and *C*). The fluctuations of the dip positions are believed to result from experimental errors, such as those occurring in lipid concentration determinations and the control of sample thermal history.

DHE intensity dips over a wide range of sterol concentrations

Fig. 4 shows that DHE intensity dips were observable at 7.7, 9.0, 9.6, 10.8, 11.8, 14.7, 15.8, 20.3, 22.6, 25.3, 33.3, 43.0,

TABLE 2 Reproducibility of DHE intensity dips measured at 35°C

DHE dip in the neighborhood of mol% of total sterol	Reproducibility			
	7 days		28 days	
	DHE/Erg/DMPC*	DHE/Chol/DMPC#	DHE/Erg/DMPC*	DHE/Chol/DMPC#
20	100%	100%	100%	100%
22.2	23%	100%	0	100%
25	100%	100%	100%	100%
26.5	15%	37%	7%	6%

*The data were determined from 13 sets of independently prepared samples incubated at room temperature.
#The data were determined from 16 sets of independently prepared samples incubated at room temperature.

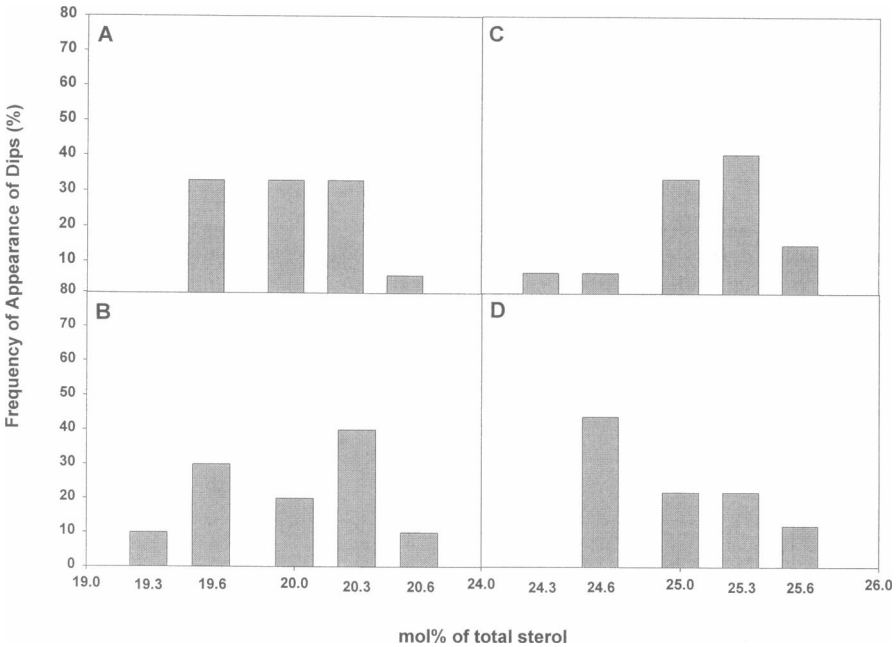

FIGURE 3 Distribution of DHE intensity dips observed in the neighborhood of 20 (*A* and *B*) and 25 (*C* and *D*) mol% total sterol in DHE/cholesterol/DMPC (*A* and *C*) and DHE/ergosterol/DMPC (*B* and *D*) mixtures. The frequency of appearance of dips was determined from 13 independently prepared samples for *B* and *D* and from 16 samples for *A* and *C*. The height of the column represents the frequency of appearance of the dip at the sterol concentration indicated underneath. The sample incubation time was 28 days. The average dip positions and their standard deviations were (*A*) 20.0 ± 0.32 mol%, (*B*) 20.0 ± 0.39 mol%, (*C*) 25.1 ± 0.33 mol%, and (*D*) 25.0 ± 0.37 mol% total sterol.

and 50.0 mol% total sterol in DHE (fixed at 0.5 mol%)/cholesterol/DMPC bilayers at 35°C. These dips are in good agreement with the critical sterol mole fractions predicted by either the hexagonal or centered rectangular superlattice model (Table 1). Despite a 3 mol% deviation, the 43 mol% dip is still considered to be in good agreement with the theoretical value (40 mol%) because this dip region is broad. The overall intensity profile, in the range of 8–53 mol% total sterol, is similar to that obtained from DHE/DMPC mixtures (Chong, 1994), except that the dips at 33.3 and 50.0 mol% total sterol (Fig. 3) are not so shallow and broad as those in DHE/DMPC mixtures (Chong, 1994). Another point is that a dip at ~40 mol% was not observed in DHE/DMPC mixtures after the samples were incubated at room temperature for 14 days (Chong, 1994). In contrast, a broad dip at ~43.0 mol% is clearly discernible in DHE/cholesterol/DMPC mixtures (Fig. 4), even after the samples are incubated at room temperature for 4 weeks. According to the calculated critical concentrations (Table 1), one would expect a single dip at 10 mol%, whereas in Fig. 4 two dips close to 10 mol% were detected, one at 9.6 mol% and the other at 10.8 mol%. The physical origin of the extra dip is not clear. This, however, does not affect the conclusion on the formation of sterol superlattices, because for the purpose of comparison between the theoretical and observed values, the dips in the low concentration region (<11 mol%) are not as useful as those in the intermediate concentration region (17–55 mol% sterol) (Chong, 1994). The dips in the intermediate concentration region are more separated and can more easily be recognized.

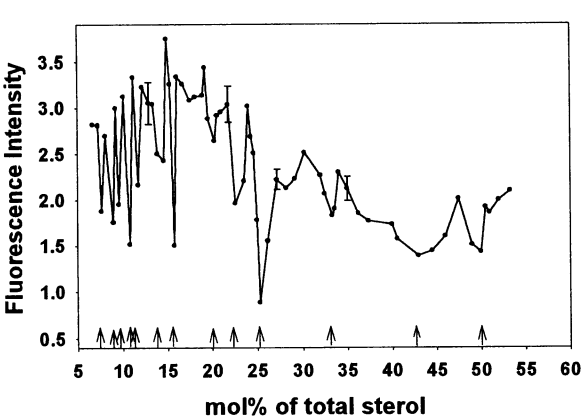

FIGURE 4 Effect of total sterol content on the DHE fluorescence intensity (measured at 35°C) at 378 nm in DHE/cholesterol/DMPC mixtures with DHE fixed at 0.5 mol%. The sample incubation time was 28 days.

DHE lifetime dips

The emission decay of DHE fluorescence in DHE (fixed at 0.5 mol%)/ergosterol/DMPC and in DHE (fixed at 0.5 mol%)/cholesterol/DMPC multilamellar vesicles at 35°C was determined by phase and modulation measurements using modulation frequencies ranging from 30 to 200 MHz. The data are best fit by a two-exponential decay law: $F(t) = \alpha_1 \exp(-t/\tau_1) + \alpha_2 \exp(-t/\tau_2)$, where α_i and τ_i are the preexponential factor and lifetime, respectively, for the *i*th component. The fitted decay parameters obtained from DHE/ergosterol/DMPC mixtures, along with the target function values, χ^2, at the end of each optimization, are listed in Table 3, where f_i is the fraction of the total fluorescence intensity derived from the *i*th component ($f_1 = \alpha_1\tau_1/(\alpha_1\tau_1 + \alpha_2\tau_2)$ and $f_2 = 1 - f_1$) and $\langle\tau\rangle$ is the average lifetime calculated from the equation $\langle\tau\rangle = f_1\tau_1 + f_2\tau_2$. The average lifetime of DHE fluorescence exhibits sharp dips at 14.3, 15.8, 20.3, and 25.0 mol% total sterol in DHE/ergos-

TABLE 3 Fitted decay parameters of DHE fluorescence in DHE/ergosterol/DMPC multilamellar (with DHE fixed at 0.5 mol%) vesicles at 35°C

Mol% of total sterol	τ_1 (ns)	f_1	α_1	τ_2 (ns)	χ^2	$\langle\tau\rangle$ (ns)
11.3	0.71 ± 0.02	0.64 ± 0.01	0.85	2.30 ± 0.07	3.78	1.28 ± 0.04
12.3	0.53 ± 0.04	0.42 ± 0.05	0.69	1.67 ± 0.12	2.94	1.19 ± 0.11
13.5	0.63 ± 0.04	0.54 ± 0.05	0.78	1.87 ± 0.19	3.89	1.20 ± 0.13
14.0	1.43 ± 0.09	0.68 ± 0.07	0.42	0.49 ± 0.07	2.96	1.13 ± 0.12
14.3	0.76 ± 0.14	0.70 ± 0.23	0.80	1.92 ± 0.22	2.32	1.11 ± 0.49
14.7	1.24 ± 0.03	0.69 ± 0.07	0.46	0.48 ± 0.26	2.75	1.00 ± 0.13
15.4	0.93 ± 0.07	0.77 ± 0.14	0.88	2.13 ± 0.65	2.98	1.21 ± 0.36
15.8	1.14 ± 0.06	0.88 ± 0.08	0.66	0.32 ± 0.19	4.68	1.04 ± 0.11
16.2	0.81 ± 0.06	0.63 ± 0.11	0.84	1.87 ± 0.70	2.00	1.20 ± 0.35
17.6	0.78 ± 0.06	0.71 ± 0.13	0.88	2.20 ± 0.53	3.63	1.19 ± 0.34
19.0	1.41 ± 0.12	0.73 ± 0.12	0.54	0.62 ± 0.10	1.74	1.20 ± 0.21
19.3	0.63 ± 0.05	0.48 ± 0.07	0.71	1.71 ± 0.19	3.46	1.19 ± 0.16
19.6	0.47 ± 0.18	0.28 ± 0.02	0.57	1.59 ± 0.02	4.84	1.28 ± 0.06
20.0	0.51 ± 0.06	0.35 ± 0.06	0.72	1.34 ± 0.01	4.44	1.05 ± 0.09
20.3	1.21 ± 0.08	0.79 ± 0.08	0.55	0.39 ± 0.12	3.25	1.04 ± 0.12
20.6	1.21 ± 0.05	0.85 ± 0.04	0.56	0.28 ± 0.13	4.55	1.07 ± 0.07
21.0	1.40 ± 0.67	0.74 ± 0.06	0.52	0.53 ± 0.04	3.20	1.17 ± 0.50
21.8	1.48 ± 0.08	0.74 ± 0.04	0.50	0.52 ± 0.04	5.28	1.23 ± 0.09
22.6	0.57 ± 0.02	0.48 ± 0.02	0.75	1.86 ± 0.10	2.59	1.24 ± 0.07
24.0	0.88 ± 0.08	0.51 ± 0.11	0.68	1.78 ± 0.16	2.23	1.32 ± 0.24
24.3	0.75 ± 0.07	0.53 ± 0.11	0.74	1.85 ± 0.07	4.24	1.27 ± 0.23
24.6	1.28 ± 0.07	0.82 ± 0.07	0.59	0.41 ± 0.13	4.78	1.12 ± 0.11
25.0	0.61 ± 0.07	0.56 ± 0.11	0.76	1.58 ± 0.37	2.35	1.04 ± 0.25
25.6	1.43 ± 0.01	0.65 ± 0.01	0.48	0.69 ± 0.49	2.13	1.17 ± 0.17
26.2	0.86 ± 0.06	0.69 ± 0.07	0.87	2.53 ± 0.13	5.58	1.38 ± 0.20
27.2	0.88 ± 0.03	0.70 ± 0.04	0.87	2.49 ± 0.03	1.25	1.36 ± 0.11

terol/DMPC mixtures (indicated by *arrows* in Fig. 5 *A*) and at 20.3, 22.6 and 24.6 mol% total sterol in DHE/cholesterol/DMPC mixtures (Fig. 5 *B*). These mole fractions are identical or close to the theoretical values predicted for sterol regular distribution in hexagonal or centered rectangular superlattices (Table 1). No DHE fluorescence lifetime dip was observed at 22.2 mol% in DHE/ergosterol/DMPC mixtures (Fig. 5 *A*). This is consistent with the observation that under the similar incubation conditions (28–33 days at room temperature), no DHE intensity dip at 22.2 mol% total sterol was observed (Fig. 2 *D*), possibly because the centered rectangular superlattice at 22.2 mol% is metastable, as discussed earlier.

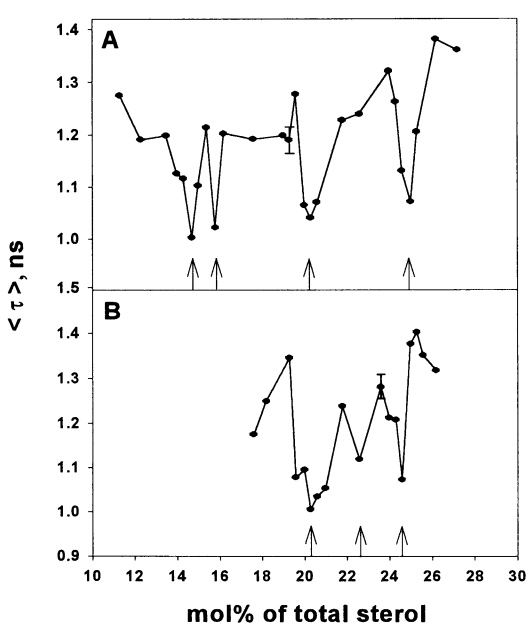

FIGURE 5 Effect of total sterol mole fraction on the average lifetime (measured at 35°C) of DHE fluorescence, $\langle\tau\rangle$, in (*A*) DHE/ergosterol/DMPC and (*B*) DHE/cholesterol/DMPC mixtures. DHE was fixed at 0.5 mol%. The sample incubation time was 33 days.

DHE anisotropy peaks

Fig. 6 shows the effect of total sterol content on the steady-state anisotropy of DHE fluorescence (measured at 35°C) in DHE (fixed at 3 mol%)/cholesterol/DMPC multilamellar vesicles. Local maxima were detected at 6.0, 10.2, 11.8, 12.3, 13.5, 15.8, 20.3, 22.2, 24.6, 26.5, 32.0, 35.0, 40.0, and 50 mol% total sterol, as indicated by arrows in Fig. 6. These mole fractions, except for 26.5 mol%, match the theoretically predicted critical mole fractions for sterol regular distribution in either hexagonal or centered rectangular superlattices (Table 1). Peaks at 29.2 and 19.0 mol% (Fig. 6) are not considered real peaks because their peak heights are significantly smaller than the experimental errors. Moreover, according to the calculated critical concentrations (Table 1), one would expect a single peak at 33.3 mol%, whereas in Fig. 6 two peaks were detected, one at 32.0 and

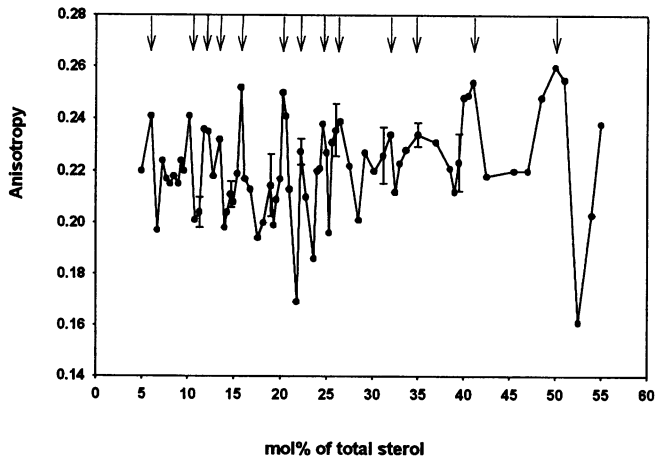

FIGURE 6 Effect of total sterol content on the steady-state anisotropy of DHE fluorescence (measured at 35°C) in DHE/cholesterol/DMPC mixtures with DHE fixed at 3 mol%. The sample incubation time was 14 days.

the other at 35.0 mol%. Although we do not know the physical origin of the extra peak, these two observed peak positions are fairly close to the predicted critical sterol mole fraction, i.e., 33.3 mol%.

When the DHE content is lowered from 3 mol% to 0.5 mol% in DHE/cholesterol/DMPC mixtures, the anisotropy maximum is still observable, as illustrated by the 19.6 mol% peak shown in Fig. 7 *A*. This result indicates that an anisotropy peak appears as long as the total sterol mole fraction reaches the critical concentrations, irrespective of the DHE content. Using the anisotropy data shown in Fig. 7 *A* and the average lifetimes presented in Table 3 and assuming that the emission decay is single exponential and that the fluorophore is spherical, we have calculated the rotational relaxation times, ρ, of DHE at different total sterol mole fractions (Fig. 7 *B*) using the Perrin equation (Perrin, 1936) $\rho = \langle\tau\rangle/[(r_o/r) - 1]$, where r is the measured steady-state anisotropy and r_o is the limiting anisotropy ($r_o = 0.37$; Chong and Thompson, 1986). The rotational relaxation time of DHE reaches a local maximum at 19.6 mol% total sterol, a concentration close to the critical sterol mole fraction of 20 mol%. Although the above assumptions are an oversimplification, the rotational relaxation times are useful for the purpose of comparison, showing the rotational rate of DHE reaching a local minimum at critical sterol mole fractions.

DHE anisotropy peaks also occur in the liquid-crystalline state of DHE (fixed at 0.5 mol%)/cholesterol/DPPC bilayers (Fig. 8). In this system, major anisotropy peaks were detected at 20.3, 22.3, 24.6, and 26.0 mol% total sterol at 56°C. This is the first time that fluorescence peaks/dips were detected near the critical sterol mole fractions when DPPC was the matrix lipid. This result agrees with our earlier prediction that cholesterol tends to be surrounded by the matrix DPPC lipids (Sugar et al., 1991), because differential scanning calorimetric data for cholesterol in DPPC vesicles showed a negative deviation from ideality (Mabrey et al., 1978).

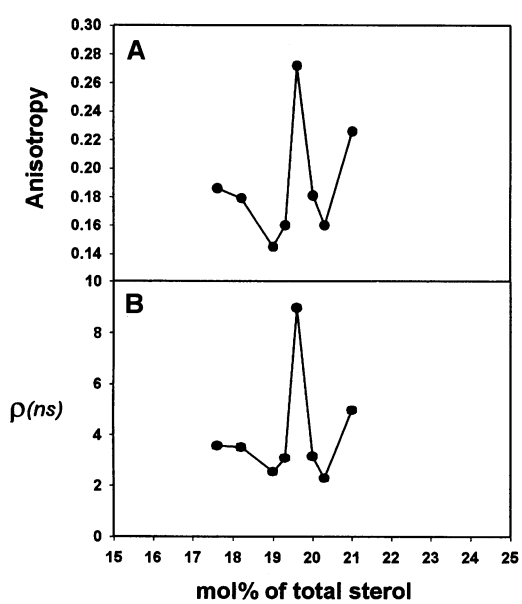

FIGURE 7 (*A*) Steady-state anisotropy (measured at 35°C) of DHE fluorescence in the neighborhood of 20 mol% total sterol in DHE/cholesterol/DMPC mixtures with DHE fixed at 0.5 mol%. The sample incubation time was ~6 weeks. (*B*) Rotational relaxation times, ρ, of DHE as a function of total sterol content. ρ was calculated from the steady-state anisotropy values, r, shown in *A* and the average lifetime values listed in Table 3, from the Perrin equation $\rho = \langle\tau\rangle/[(r_o/r) - 1]$, where the lower limiting anisotropy $r_o = 0.37$.

DISCUSSION

Regular distribution of fluorescent lipid analogs in liquid-crystalline phospholipid bilayers has previously been reported in PyrPC/PC (phosphatidylcholine) (Somerharju et al., 1985; Kinnunen et al., 1987; Tang and Chong, 1992) and DHE/PC (Chong, 1994; Chong et al., 1996a,b) membrane systems. Both the pyrene moiety of PyrPC and the tetracyclic ring of DHE are bulky and rigid. Thus the similarity in the behavior of lipid lateral organization be-

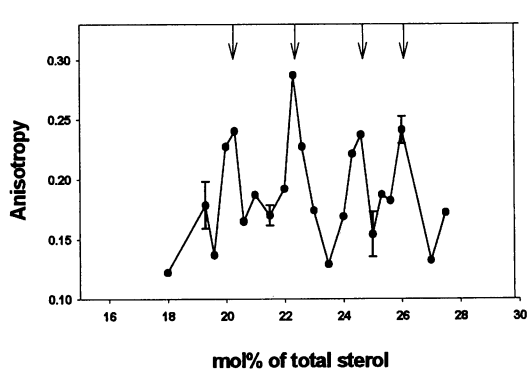

FIGURE 8 Effect of total sterol content on the steady-state anisotropy of DHE fluorescence (measured at 56°C) in DHE/cholesterol/DPPC multilamellar vesicles with DHE fixed at 0.5 mol%. The sample incubation time was 14 days.

tween PyrPC/DMPC and DHE/DMPC suggests a general phenomenon. That is, guest lipid molecules with a cross-sectional area significantly larger (or smaller) than the cross-sectional area of the acyl chain in the matrix lipid tend to maximally separate and form regularly distributed patterns. Because DHE resembles cholesterol and ergosterol in possessing a rigid tetracyclic ring, we expect that, in bilayers composed of DHE/cholesterol/PC or DHE/ergosterol/PC, a DHE dip is observable whenever the mole fraction of the total sterol is at a critical sterol mole fraction, regardless of the ratio of DHE to cholesterol or the ratio of DHE to ergosterol. Our present data (Figs. 1, 6, and 7) showed that this is indeed the case. Despite the subtle differences in sterol conformations among DHE, ergosterol, and cholesterol, fluorescence intensity dips and anisotropy peaks are observable in DHE/cholesterol/DMPC, DHE/ergosterol/DMPC, and DHE/cholesterol/DPPC mixtures whenever the total sterol mole fraction is close to the critical mole fractions predicted for sterols regularly distributed into superlattices (Table 1). This supports the idea (Chong, 1994) that sterols are regularly distributed because of the presence of a bulky and rigid tetracyclic ring.

Although DHE, ergosterol, and cholesterol can be regularly distributed in liquid-crystalline DMPC and DPPC bilayers (Figs. 1, 2, 4–8), subtle differences in sterol structures cause changes in the molecular details of sterol lateral organization. For example, in addition to the fluorescence dips corresponding to hexagonal superlattices, we have observed intermediate dips at concentrations corresponding to centered rectangular superlattices (e.g., the 22.2 mol% dip; Table 1). However, the 22.2 mol% dip in DHE/ergosterol/DMPC mixtures becomes diminished after a long incubation (~28 days) at room temperature (Fig. 2), whereas the same dip in DHE/cholesterol/DMPC mixtures remains discernible after a long incubation. Apparently, in DHE/ergosterol/DMPC mixtures, the centered rectangular superlattice detected at 22.2 mol% is metastable. Similar phenomena were noticed in DHE/DMPC binary mixtures, from which a shallow intermediate dip between two sharp DHE dips at 20 and 25 mol% was detectable for samples incubated for 2 days at room temperature; but this intermediate dip disappeared after a much longer incubation (Chong, unpublished results). Furthermore, in DHE/DMPC binary mixtures, a 40 mol% dip was not detectable after 14 days' incubation, whereas the 33 and 51 mol% dips were discernible (Chong, 1994). Because of the lack of a 40 mol% dip, it was determined (Chong, 1994) that the extended hexagonal superlattice model best describes the sterol lateral organization in DHE/DMPC mixtures. In contrast, our present study indicated that, in DHE/cholesterol/phosphatidylcholine mixtures, the 22.2 mol% DHE intensity/lifetime dips and the 40 mol% anisotropy peak were clearly discernible, even for samples incubated for more than 2 weeks (Figs. 2 and 4–8). Thus lateral organization models derived from cholesterol/PC bilayers (e.g., Virtanen et al., 1995) are not necessarily applicable to DHE/PC or ergosterol/PC bilayers. However, our data do agree with the results of Virtanen et al. (1995) in that both hexagonal and centered rectangular superlattices are required to describe the lateral organization of cholesterol in PC bilayers. This means that, at critical concentrations that are characteristic of both hexagonal and centered rectangular superlattices, two types of regular distributions may coexist.

The finding that subtleties in the differences of sterol chemical structures lead to differences in sterol lateral organization is new and may be biologically important. Subtleties in the differences of sterol chemical structures have previously been related to other physical properties of sterols in cells and in lipid bilayers. For example, lanosterol is more mobile in lipid bilayers than cholesterol (Yeagle et al., 1977) because the α-methyl group at the C-14 position in the tetracyclic ring of lanosterol prevents the close contact between the *sn*-1 acyl chain of the phospholipid and the α-face of the lanosterol ring system (Huang and Mason, 1982). Kan and Bittman (1991) showed that sitosterol and cholesterol have different spontaneous rates of sterol exchange between bilayers, with the rate impeded by the 24α-ethyl group of sitosterol. Chen and Bittman (1977) demonstrated that the antifungal drug amphotericin B (AmB) binds faster to ergosterol than to cholesterol in DMPC vesicles because of the presence of the Δ^7 double bond in ergosterol. Recently, Haynes et al. (1996) demonstrated the lack of the AmB-induced second phase from the AmB-resistant *C. neoformans* strains in the time profile of 1-[4-(trimethylammonia)phenyl]-6-phenylhexa-1,3,5-triene (TMA-DPH) fluorescence intensity, suggesting that the AmB-resistant strain is not able to form transmembrane pores because the AmB-resistant strain contains an aberrant Δ^8 (instead of the normal Δ^7) double bond in its ergosterol (Kelley et al., 1994). All of these findings echo the idea previously proposed by Yeagle (1993) that although sterols play analogous roles from one type of cell to another, different cells have different sterol structures to provide a finely tuned recognition system for biological purposes.

In the sterol regular distribution model (Chong, 1994), we postulated that, in the regular region, sterol molecules are not embedded as deep in the bilayer. As a result, sterol molecules in the regular region are expected to experience a higher dielectric constant than sterol molecules in the irregular region. If so, both intensity and lifetime of DHE fluorescence should reach a local minimum (a dip) at critical sterol mole fractions because DHE fluorescence is known to decrease with increasing dielectric constant of the medium (Schroeder et al., 1987) and because the size of the regular region reaches a local maximum at critical mole fractions (Sugar et al., 1994). This assertion is fully supported by the DHE intensity (Figs. 1, 2, and 4) and lifetime (Fig. 5) data presented in this study. Both parameters display a local minimum at critical sterol mole fractions (Table 1). Note that this assertion has previously been supported by the acrylamide quenching of DHE fluorescence in DHE/DMPC mixtures (Chong et al., 1996a,b). The quenching rate constant was found to reach a local maximum at critical sterol mole fractions, indicating that DHE becomes more acces-

sible to the water-soluble quencher, acrylamide, at critical mole fractions.

Membrane cholesterol content is known to affect a number of cellular membrane activities, including endocytosis (Heiniger et al., 1976), lymphocyte capping (Hoover et al., 1983), cell adhesion (Broadley et al., 1991), platelet aggregation (Mcleod et al., 1982), the activities of membrane-bound proteins (e.g., Whetton and Houslay, 1983), and the infectivities of retrovirus (Pal et al., 1983). These effects have frequently been interpreted to be a result of cholesterol-induced changes in membrane fluidity. "Membrane fluidity" is a term that denotes the structural and dynamic properties (membrane order and rates of motion, respectively) that determine the motions of molecules in the membrane. Because motions of molecules in the membrane require membrane free volume and because the fluidity of a liquid is a strong function of volume (Bingham and Kinney, 1940), "membrane fluidity" may be better referred to as the free volume available for the motions of molecules in the membrane. Therefore, to improve our understanding of the structure-function relationship of membrane cholesterol, it is necessary to understand how variations in membrane cholesterol content change membrane free volume.

Our previous pressure study (Chong et al., 1994) showed that the membrane free volume reaches a local minimum at critical PyrPC mole fractions in DMPC vesicles. Furthermore, computer simulation data (Sugar et al., 1994) showed that regular and irregular regions coexist and that the ratio of the regular to irregular areas reaches a local maximum at critical mole fractions and a local minimum at noncritical mole fractions. These physical properties should apply, in principle, to sterol/PC mixtures. Because there are many critical mole fractions over a wide range of sterol concentrations (Chong, 1994), we proposed (Chong, 1994) that membrane free volume should vary with sterol content in an alternating manner with a local minimum in membrane free volume at critical sterol mole fractions.

This concept has recently been tested by using a membrane probe, diphenylhexatriene (DPH), in cholesterol/DMPC multilamellar vesicles (Chong, 1996; Chong et al., 1996a,b). The steady-state polarization of DPH fluorescence reflects mainly the molecular order of lipid acyl chains (Chen et al., 1977; Jahnig, 1979). If membrane free volume reaches a local minimum at a critical sterol mole fraction, DPH polarization should be higher at critical cholesterol mole fractions than at their neighboring noncritical mole fractions. We have demonstrated that, although the lifetime of DPH varies little with sterol content over the sterol mole fraction range examined (Chong et al., 1996a), DPH polarization exhibits local maxima at sterol mole fractions near 20, 22.2, and 25 mol% total sterol (Chong, 1996; Chong et al., 1996a,b). These concentrations are the critical mole fractions predicted for cholesterol regularly distributed in diacylphosphatidylcholine bilayers (Table 1). This finding is consistent with the idea of a biphasic change in membrane free volume in the vicinity of a critical sterol mole fraction (Chong, 1994). However, DPH is a free probe, not a sterol. DPH fluorescence polarization may be influenced by the partitioning of the probe between various microdomains in the membrane and may depend on its orientation with respect to the membrane normal (Davenport et al., 1985). These concerns make it difficult to understand DPH signal response.

In the present study, DHE is used as both a lipid component and a fluorescent probe. This approach alleviates the above-mentioned problems associated with DPH. DHE data showed anisotropy peaks at many critical sterol mole fractions in DHE/cholesterol/DMPC and DHE/cholesterol/DPPC bilayers (Figs. 6–8). The calculated rotational relaxation times, which are inversely proportional to the rotational rate, also showed a local maximum at a critical sterol mole fraction (Fig. 7 *B*). Thus these data provide strong evidence that the membrane free volume available for the rotation of sterol molecules varies periodically with the sterol mole fraction in the membrane, reaching a local minimum at the critical sterol mole fractions where the regularly distributed areas are at a maximum.

Based on DPH and DHE anisotropy data and previous knowledge of membrane dynamics (reviewed in Schroeder et al., 1991), we propose here that cholesterol modulates membrane free volume by 1) condensing its neighboring lipid acyl chains (a well-known phenomenon in the literature) and by 2) varying the size of regularly distributed lipid areas (a new concept). In our opinion, this concept gives a more accurate physical picture of how cholesterol alters membrane free volume. In view of the fact that under physiological conditions the cholesterol content in cell membranes fluctuates by only a few percent (Quintao et al., 1971; Alvarez et al., 1993), it is of importance to pay special attention to the "local" cholesterol concentration effect on membrane properties, especially those known to be influenced by membrane free volume.

In summary, our present data have provided evidence that DHE, ergosterol, and cholesterol can be regularly distributed in three-component liquid-crystalline PC bilayers. The data also verify the physical properties predicted by the sterol regular distribution model (Chong, 1994). Note that evidence for sterol regular distribution has been found not only in PC but also in sphingomyelin (SPM) bilayers (Chong et al., 1996a,b). Cholesterol, SPM, and PC are the major lipid components in mammalian plasma membranes, in which cholesterol/SPM/PC enriched domains are likely to occur (e.g., Lentz et al., 1980). Within these domains, lipids may be regularly distributed as superlattices, in coexistence with irregularly distributed areas (Fig. 9). The ratio of regular to irregular regions, as well as the membrane free volume, should vary with the cholesterol/phospholipid molar ratio according to the principles of lipid regular distribution (Sugar et al., 1994; Chong et al., 1994). The regions of lipid regular distribution can be considered as microdomains within the cholesterol/phospholipid-enriched domains in the plasma membrane (Fig. 9). Microdomains are local structures; thus their existence should not be

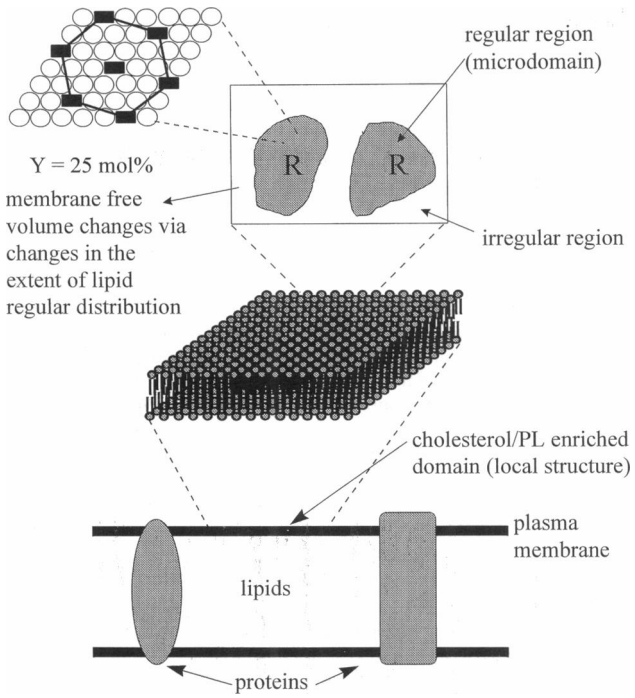

FIGURE 9 A schematic diagram showing a putative biological role of membrane cholesterol. The dark squares in the hexagonal lattice represent sterol molecules. The open circles are phospholipid hydrocarbon chains.

greatly affected by the presence of membrane proteins, the heterogeneity of membrane lipids, or cytoskeletal structures.

We thank Professor T. E. Thompson for his suggestion of the studies on DHE/cholesterol/PC mixtures.

This work was supported by the American Heart Association (95010730) and by Temple University Research Incentive Funds.

REFERENCES

Almeida, P. F. F., W. L. C. Vaz, and T. E. Thompson. 1992. Lateral diffusion in the liquid phases of dimyristoylphosphatidylcholine/cholesterol lipid bilayers: a free volume analysis. *Biochemistry.* 31: 6739–6747.

Alvarez, E., V. Ruiz-Gutierrez, C. S. Maria, and A. Machado. 1993. Age-dependent modification of lipid composition and lipid structural order parameter of rat peritoneal macrophage membranes. *Mech. Ageing Dev.* 71:1–12.

Bar, L. K., P. L.-G. Chong, Y. Barenholz, and T. E. Thompson. 1989. Spontaneous transfer between phospholipid bilayers of dehydroergosterol, a fluorescent cholesterol analog. *Biochim. Biophys. Acta.* 983: 109–112.

Bartlett, G. R. 1959. Phosphorus assay in column chromatography. *J. Biol. Chem.* 234:466–468.

Bingham, E. C., and P. W. Kinney. 1940. The relation of fluidity to volume in organic liquids. *J. Appl. Phys.* 11:192–202.

Broadley, C., E. Dawidowicz, P. L.-G. Chong, and R. Hoover. 1991. Modulation of membrane cholesterol levels: effects on endothelial cell function. *Exp. Cell Res.* 193:144–150.

Chen, W. C., and R. Bittman. 1977. Kinetics of association of amphotericin B with vesicles. *Biochemistry.* 16:4145–4149.

Chen, L. A., R. E. Dale, S. Roth, and L. Brand. 1977. Nanosecond time-dependent fluorescence depolarization of diphenylhexatriene in dimyristoyllecithin vesicles and the determination of "microviscosity." *J. Biol. Chem.* 252:2163–2169.

Chong, P. L.-G. 1994. Evidence for regular distribution of sterols in liquid crystalline phosphatidylcholine bilayers. *Proc. Natl. Acad. Sci. USA.* 91:10069–10073.

Chong, P. L.-G. 1996. Membrane free volume variation with bulky lipid concentration by regular distribution: a functionally important property explored by pressure studies of phosphatidylcholine bilayers. *In* High Pressure Effects in Molecular Biophysics and Enzymology. J. L. Markley, D. B. Northrop, and C. A. Royer, editors. Oxford University Publishing, New York. 298–313.

Chong, P. L.-G., F. Liu, M. M. Wang, K. Truong, I. P. Sugar, and R. E. Brown. 1996a. Fluorescence evidence for cholesterol regular distribution in phosphatidylcholine and in sphingomyelin lipid bilayers. *J. Fluorescence.* 6:221–230.

Chong, P. L.-G., D. Tang, and I. P. Sugar. 1994. Exploration of physical principles underlying lipid regular distribution: effects of pressure, temperature, and radius of curvature on E/M dips in pyrene-labeled PC/DMPC binary mixtures. *Biophys. J.* 66:2029–2038.

Chong, P. L.-G., and T. E. Thompson. 1986. Depolarization of dehydroergosterol in phospholipid bilayers. *Biochim. Biophys. Acta.* 863:53–62.

Chong, P. L.-G., M. M. Wang, F. Liu, K. Truong, A. A. Golsorkhi, I. P. Sugar, and R. E. Brown. 1996b. Fluorescence evidence for cholesterol regular distribution in phosphatidylcholine and in sphingomyelin lipid bilayers. Proceeding of Fluorescence Detection IV. *SPIE.* 2705: 143–154.

Davenport, L., R. E. Dale, R. H. Bisby, and R. B. Cundall. 1985. Transverse location of the fluorescent probe 1,6-diphenyl-1,3,5-hexatriene in model lipid bilayer membrane systems by resonance excitation energy transfer. *Biochemistry.* 24:4097–4108.

Delseth, C., Y. Kashman, and C. Djerassi. 1979. Ergosta-$\Delta^{5,7,9(11),22}$-tetraen-3β-ol and its 24-ζ-ethylhomolog, two new marine sterols from the red sea sponge, *Biemna fortis. Helv. Chim. Acta.* 62:2037–2045.

Haynes, M. P., P. L.-G. Chong, H. R. Buckley, and R. A. Pieringer. 1996. Fluorescence studies on the molecular action of amphotericin B on susceptible and resistant fungal cells. *Biochemistry.* 35:7983–7992.

Heiniger, H. J., A. A. Kandustch, and H. W. Chen. 1976. Depletion of L-cell sterol depresses endocytosis. *Nature.* 263:515–517.

Hoover, R. L., E. A. Dawidowicz, J. M. Robinson, and M. J. Karnovsky. 1983. Role of cholesterol in the capping of surface immunoglobulin receptors on murine lymphocytes. *J. Cell Biol.* 97:73–80.

Huang, C., and J. T. Mason. 1982. Complementary packing of phosphoglyceride and cholesterol molecules in the bilayer. *In* Membrane and Transport, Vol. 1. A. N. Martosoni, editor. Plenum Publishing, New York. 15–23.

Hui, S. W. 1993. Visualization of cholesterol domains in model membranes. *In* Cholesterol in Membrane Models. L. Finegold, editor. CRC Press, Boca Raton, FL. 159–173.

Hyslop, P. A., B. Morel, and R. D. Sauerheber. 1990. Organization and interaction of cholesterol and phosphatidylcholine in model bilayer membranes. *Biochemistry.* 29:1025–1038.

Ipsen, J. H., G. Karlstrom, O. G. Mouritsen, H. Wennerstrom, and M. J. Zuckermann. 1987. Phase equilibra in the phosphatidylcholine-cholesterol system. *Biochim. Biophys. Acta.* 905:162–172.

Jahnig, F. 1979. Structural order of lipids and proteins in membranes: evaluation of fluorescence anisotropy data. *Proc. Natl. Acad. Sci. USA.* 76:6361–6365.

Kan, C. C., and R. Bittman. 1991. Spontaneous rates of sitosterol and cholesterol exchange between phospholipid vesicles and between lysophospholipid dispersions: evidence that desorption rate is impeded by the 24α-ethyl group of sitosterol. *J. Am. Chem. Soc.* 113:6650–6656.

Kao, Y. L., P. L.-G. Chong, and C.-h. Huang. 1990. Time-resolved fluorometric and differential scanning calorimetric investigation of dehydroergosterol in 1-stearoyl-2-caprylphosphatidylcholine bilayers. *Biochemistry.* 29:1315–1322.

Kelly, S. L., D. C. Lamb, M. Taylor, A. J. Corran, B. C. Baldwin, and W. G. Powderly. 1994. Resistance to amphotericin B associated with defective sterol Δ^{8-7} isomerase in a *Cryptococcus neoformans* strain from an AIDS patient. *FEMS Microbiol. Lett.* 122:39–42.

Kinnunen, P. K. J., A. Tulkki, H. Lemmetyinen, J. Paakkola, and A. Virtanen. 1987. Characteristics of excimer formation in Langmuir-

Blodgett assemblies of 1-palmitoyl-2-pyrenedecanoylphosphatidylcholine and dipalmitoylphosphatidylcholine. *Chem. Phys. Lett.* 136: 539–545.

Lakowicz, J. R., H. Cherek, and A. Balter. 1981. Correction of timing errors in photomultiplier tubes used in phase-modulation fluorometry. *J. Biochem. Biophys. Methods.* 5:131–146.

Lentz, B. R., D. A. Barrow, and M. Hoechli. 1980. Cholesterol-phosphatidylcholine interactions in multilamellar vesicles. *Biochemistry.* 19:1943–1954.

Lin, H.-n., and C.-h. Huang. 1988. Eutectic phase behavior of 1-stearoyl-2-caprylphosphatidylcholine and dimyristoylphosphatidylcholine mixtures. *Biochim. Biophys. Acta.* 946:178–184.

Mabrey, S., P. L. Mateo, and J. M. Sturtevant. 1978. High-sensitivity scanning calorimetric study of mixtures of cholesterol with dimyristoyl- and dipalmitoylphosphatidylcholines. *Biochemistry.* 17:2464–2468.

Mason, J. T. 1994. Properties of phosphatidylcholine bilayers as revealed by mixed-acyl phospholipid fluorescent probes containing *n*-(9-anthroyloxy) fatty acids. *Biochim. Biophys. Acta.* 1194:99–108.

Matteo, C. R., A. U. Acuna, and J.-C. Bronchon 1995. Liquid-crystalline phases of cholesterol/lipid bilayers as revealed by the fluorescence of trans-parinaric acid. *Biophys. J.* 68:978–987.

Mcleod, A. J., K. E. Suckling, P. L. Walton, and M. Johnson. 1982. Effects of in vitro incorporation of cholesterol and cholesterol analogues into rat platelets. *Biochim. Biophys. Acta.* 688:581–585.

McMullen, T. P. W., and R. N. McElhaney. 1995. New aspects of the interaction of cholesterol with dipalmitoylphosphatidylcholine bilayers as revealed by high-sensitivity differential scanning calorimetry. *Biochim. Biophys. Acta.* 1234:90–98.

Melchior, D. L., F. J. Scavitto, and J. M. Steim. 1980. Dilatometry of dipalmitoyllecithin-cholesterol bilayers. *Biochemistry.* 19:4828–4834.

Muczynski, K. A., and W. L. Stahl. 1983. incorporation of dansylated phospholipids and dehydroergosterol into membranes using a phospholipid exchange protein. *Biochemistry.* 22:6037–6048.

Pal, R., J. R. Wiener, Y. Barenholz, and R. R. Wagner. 1983. Influence of the membrane glycoprotein and cholesterol of vesicular stomatitis virus on the dynamics of viral and model membranes. *Biochemistry.* 22: 3624–3630.

Parasassi, T., A. M. Giusti, M. Raimondi, and E. Gratton. 1995. Abrupt modifications of phospholipid bilayer properties at critical cholesterol concentrations. *Biophys. J.* 68:1895–1902.

Perrin, F. 1936. Mouvement brownien d'un ellipsoide (II). Rotation libre et dipolarisation des fluorescences. Transaction et diffusion de molecules ellipsoidoles. *J. Phys. Radium.* 7:1–44.

Quintao, E., S. M. Grundy, and E. H. Ahrens. 1971. Effects of dietary cholesterol on the regulation of total body cholesterol in man. *J. Lipid Res.* 12:233–247.

Rogers, J., A. G. Lee, and D. D. Wilton. 1979. The organisation of cholesterol and ergosterol in lipid bilayers based on studies using non-perturbing fluorescent sterol probes. *Biochim. Biophys. Acta.* 552:23–37.

Schroeder, F., Y. Barenholz, E. Gratton, and T. E. Thompson. 1987. A fluorescence study of dehydroergosterol in phosphatidylcholine bilayer vesicles. *Biochemistry.* 26:2441–2448.

Schroeder, F., J. R. Jefferson, A. B. Kier, J. Knittel, T. Scallen, W. G. Wood, and I. Hapala. 1991. Membrane cholesterol dynamics: cholesterol domains and kinetic pools. *Proc. Soc. Exp. Biol. Med.* 196: 235–252.

Somerharju, P. J., J. A. Virtanen, K. K. Eklund, P. Vainio, and P. K. J. Kinnunen. 1985. 1-Palmitoyl-2-pyrenedecanoyl glycerophospholipids as membrane probes: evidence for regular distribution in liquid-crystalline phosphatidylcholine bilayers. *Biochemistry.* 24:2773–2781.

Sugar, I. P., D. Tang, and P. L.-G. Chong. 1994. Monte Carlo simulation of lateral distribution of molecules in a two-component lipid membrane. Effect of long-range repulsive interactions. *J. Phys. Chem.* 98: 7201–7210.

Sugar, I. P., J. Zeng, and P. L.-G. Chong. 1991. Use of Fourier transforms in the analysis of fluorescence data. 3. Fluorescence of pyrene-labeled phosphatidylcholine in lipid bilayer membrane. A three-state model. *J. Phys. Chem.* 95:7524–7534.

Tang, D., and P. L.-G. Chong. 1992. E/M dips: evidence for lipids regularly distributed into hexagonal super-lattices in pyrene-PC/DMPC binary mixtures at specific concentrations. *Biophys. J.* 63:903–910.

Tang, D., W. B. van der Meer, and S.-Y. S. Chen. 1995. Evidence for a regular distribution of cholesterol in phospholipid bilayers from diphenylhexatriene fluorescence. *Biophys. J.* 68:1944–1951.

Virtanen, J., M. Ruonala, M. Vauhkonen, and P. Somerharju. 1995. Lateral organization of liquid-crystalline cholesterol-dimyristoylphosphatidylcholine bilayers. Evidence for domains with hexagonal and centered rectangular cholesterol superlattices. *Biochemistry.* 34:11568–11581

Virtanen, J. A., P. Somerharju, and P. K. J. Kinnunen. 1988. Prediction of patterns for the regular distribution of soluted guest molecules in liquid crystalline phospholipid membranes. *J. Mol. Electron.* 4:233–236.

Vist, M. R., and J. H. Davis. 1990. Phase equilibria of cholesterol/DPPC mixtures: ^{2}H-NMR and DSC. *Biochemistry.* 29:451–464.

Whetton, A. D., and M. D. Houslay. 1983. 5′-Nucleotidase is activated upon cholesterol-depletion of liver plasma membranes. *FEBS Lett.* 157: 70–74.

Yeagle, P. L. 1993. The biophysics and cell biology of cholesterol: an hypothesis for the essential role of cholesterol in mammalian cells. *In* Cholesterol in Membrane Models. L. Finegold, editor. CRC Press, Boca Raton, FL. 1–12.

Yeagle, P. L., R. B. Martin, A. K. Laka, H. K. Lin, and K. Block. 1977. Differential effects of cholesterol and lanosterol on artificial membranes. *Proc. Natl. Acad. Sci. USA.* 74:4924–4926.